

# Dissipatively stabilized quantum sensor based on indirect nuclear-nuclear interactions

Q. Chen<sup>†</sup>, I. Schwarz<sup>†</sup>, and M.B. Plenio

*Institut für Theoretische Physik, Albert-Einstein-Allee 11, Universität Ulm, 89069 Ulm, Germany*

<sup>†</sup> *These authors contributed equally to this work*

We propose to use a dissipatively engineered nitrogen vacancy (NV) center as a mediator of interaction between two nuclear spins that are protected from decoherence and relaxation of the NV. Under ambient conditions this scheme achieves highly selective high-fidelity quantum gates between nuclear spins in a quantum register even at large NV-nuclear distances. Importantly, this method allows for the use of nuclear spins as a sensor rather than a memory, while the NV spin acts as an ancillary system for the initialization and read out of the sensor. The immunity to the decoherence and relaxation of the NV center leads to a tunable sharp frequency filter while allowing at the same time the continuous collection of the signal to achieve simultaneously high spectral selectivity and high signal-to-noise ratio (SNR).

*Introduction* — The Nitrogen vacancy (NV) center is attracting increasing attention due to the possibility for creating hybrid quantum registers of nuclear spins controlled by the electron spin of the NV center [1–4] and due to its applications in nanoscale sensing [5–27]. However, for both quantum register and sensing applications, there are several outstanding challenges caused by the relaxation and decoherence processes of the NV center electron spin as these limit quantum gate fidelities on nuclear registers as well as spectral resolution, selectivity and signal to noise ratio in sensing applications. While the addition of the nuclear ancilla as long-lived memory of the NV sensor can improve spectral resolution, by extending the time interval between interrogations, e.g. in correlation spectroscopy, this comes at a price of signal to noise ratio and remains limited by the relaxation time of the NV center.

Here we address directly the challenge of the NV center decoherence and relaxation by using the NV center as a mediator to couple two nuclear spins, while eliminating the NV center and the effect of its decoherence and relaxation from the dynamics (Fig. 1a). Thus, coherent evolution between nuclear spins is achieved which is no longer limited by the NV decoherence or even relaxation. The key idea is the use of the substantial second order coupling between the nuclear spins obtained through a strongly detuned NV center which is periodically reinitialized by a dissipative process [28]. The detuning and periodical reinitialization of the NV center decouple it from the dynamics and its effect on the system can be modeled by an effective but weak dissipation process. Thus, high fidelity of selective quantum gates between the nuclear spins, as well as an improved sensing setup, are made possible even at ambient condition.

We demonstrate that the NV-mediated interaction between nuclear spins yields a dissipation-enhanced quantum sensor by considering a basic setup including a single  $^{13}\text{C}$  nuclear spin sensor nearby the shallow NV center to sense a target  $^{13}\text{C}$  spins on the diamond surface, as shown in Fig. 1b. Contrary to previous applications of nuclear spins acting as ancillary memory [19–27], the nuclear spin in our set-up serves directly as a sensor, while

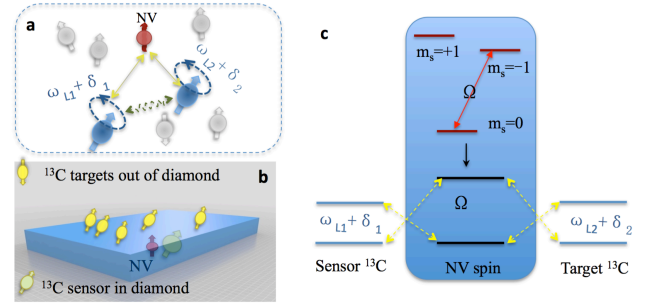


FIG. 1. (a) Illustration of the basic principle. An NV center mediates the coupling between two nuclear spins, while itself becoming decoupled from the dynamics, enabling long coherent interactions, e.g. for high fidelity selective quantum gates. Dissipation-assisted sensing set-up composed of a nuclear quantum sensor (a single  $^{13}\text{C}$  spin (green)  $\sim 1$  nm removed from the associated NV center (red)) and an NV implanted 3-4 nm below the diamond surface where the target spins reside (yellow). (b) Energy level diagram. The Rabi frequency  $\Omega$  of the MW drive is far off resonance from the Larmor frequency of the target nucleus which is on resonance with the sensor. (c) Energy level diagram. The Rabi frequency  $\Omega$  of the MW drive is far off resonance from the Larmor frequency of the target nucleus which is on resonance with the sensor.

the NV spin is an ancillary mediator of interaction, and at beginning and end serves as a means for initialization and read out of the sensor spin. The effective coupling between the two nuclear spins is controllable, which provides a tunable sharp frequency filter for achieving very high spectral resolution that is not limited by the NV decoherence and relaxation. Additionally, the signal is continuously accumulated by the nuclear sensor, with no dead-time, hence maintaining sensitivity by increasing the SNR. Furthermore our scheme does not merely measure Larmor frequency [5] but retains the option of individually addressing the nuclear spins, useful for 2D spectroscopy [20, 29, 30] and quantum registers.

*Effective master equation* — The basic setting we consider here includes a single NV center spin and two  $^{13}\text{C}$  nuclear spins. Applying a weak magnetic field  $\vec{B}_0$  lifts the degeneracy of  $|m_s = -1\rangle$  and  $|m_s = +1\rangle$  to allow for selective continuous microwave (MW) driving field of one specific electronic transition. Working in

a frame that is rotating with the MW frequency, resonant with the  $|m_s = 0\rangle \leftrightarrow |m_s = -1\rangle$  transition, the effective Hamiltonian of the NV spin is  $H_{NV} = \Omega\sigma_z$ . Here,  $\Omega$  is the Rabi frequency of the MW drive and  $\{|+_x\rangle = \frac{1}{\sqrt{2}}(|0\rangle + |-1\rangle), |-_x\rangle = \frac{1}{\sqrt{2}}(|0\rangle - |-1\rangle)\}$  are the MW dressed eigenstates. Our goal is to use such MW dressed NV center spin as a mediator for indirect coherent interactions between two nuclear spins. The interaction between the NV and a nuclear spin is given by

$$H_{intf} = S_z \vec{A}_i \cdot \vec{I}_i = S_z (a_{\parallel i} I_i^z + a_{\perp i} I_i^x), \quad (1)$$

where  $\vec{A}_i$  is the hyperfine coupling vector and the direction of  $\vec{I}_i$  is determined by the magnetic field unit vector  $\vec{b}(\theta, \phi)$ .  $S_q$  and  $I_i^q$  are the NV electronic spin and external nuclear spin operators respectively.  $\vec{A}_i = (a_{\parallel i}, a_{\perp i})$  with  $a_{\parallel i}$  and  $a_{\perp i}$  denoting the parallel and perpendicular coupling components to the nuclear spin quantization axes  $a_{\parallel i} = \vec{A}_i \cdot \vec{b}$  and  $a_{\perp i} = \sqrt{|\vec{A}_i|^2 - a_{\parallel i}^2}$ .

We derive a Lindblad master equation to describe the dynamics of the whole system  $\rho$ , which is described as  $\frac{d}{dt}\rho = -i[H'_{tot}, \rho] + \mathcal{D}[\rho]$  in which  $\mathcal{D}[\rho] = \mathcal{D}_e[\rho] + \mathcal{D}_n[\rho]$ , corresponding to the relaxation and dephasing of the electron and nuclear spins, respectively. The effective total Hamiltonian of the three spins are thus rewritten as (for details see SI [31])

$$H'_{tot} = \Omega\sigma_z + \sum_{i=1}^2 (\gamma_{ni} \vec{B}_0 \vec{I}_i + \frac{\vec{A}_i \vec{I}_i}{2}) + \sigma_x \vec{A}_i \vec{I}_i, \quad (2)$$

with  $\gamma_{ni}$  the gyromagnetic ratio of the nuclear spin. The NV center is reinitialized periodically (every  $t_{re}$ ) to the state  $|-_x\rangle$  of the dressed state basis, namely,  $\rho(Nt_{re}) \rightarrow [\text{Tr}_e \rho(Nt_{re})] \otimes |-_x\rangle\langle -_x|$ , where  $\text{Tr}_e$  denotes the partial trace over the electron spin and  $N$  is an integer.

The reinitialization of the NV results in nuclear subsystem evolution in the vicinity of the NV quasi-steady state,  $\rho_{ss}^{NV} = p_+ |+_x\rangle\langle +_x| + p_- |-_x\rangle\langle -_x|$ , in which  $p_+ = 1 - \frac{e^{-t_{re}/T_{1\rho}}}{2t_{re}/T_{1\rho}}$  when  $t_{re} \leq T_{1\rho}$  and  $p_+ = \frac{1}{2} - \frac{1-e^{-1}}{2t_{re}/T_{1\rho}}$  when  $t_{re} > T_{1\rho}$ ,  $p_- = 1 - p_+$ . Notice that the effective relaxation rate of the NV spin is determined by the lifetime  $T_{1\rho}$  and the reinitialization time  $t_{re}$ ,  $\Gamma_N = 1/T_{1\rho} + 1/t_{re}$ . We can now use the electron spin as a bus to mediate the nuclear coupling [4, 28], if the relevant energy scales satisfy  $\Omega, \gamma_{n1}B_0, |\Omega - \gamma_{n1}B_0| \gg |\vec{A}_i|$ . The Schrieffer-Wolff transformation for open systems [32, 33] then allows for the derivation of an effective Liouvillian (see SI for details) [31] for the nuclear subsystem  $\rho_n$

$$\frac{d}{dt}\rho_n = -i[H_{eff}, \rho_n] + \mathcal{D}_n[\rho_n] + \mathcal{D}_{eff}[\rho_n]. \quad (3)$$

Here the coherent Hamiltonian is

$$H_{eff} \approx \sum_{i=1,2} (\omega_{Li} + \delta_i) I_i^z + p A_{wo} (I_1^+ I_2^- + I_1^- I_2^+), \quad (4)$$

in which we have  $p = p_+ - p_-$ ,  $\omega_{Li} = \gamma_{ni}B_0$  and

$$\delta_1 \approx \frac{a_{\parallel i}}{2} - \frac{a_{\perp i}^2}{16} \left( \frac{\Delta_{-i}}{\Delta_{-i}^2 + (\frac{\Gamma_N}{2})^2} + \frac{\Delta_{+i}}{\Delta_{+i}^2 + (\frac{\Gamma_N}{2})^2} \right), \quad (5)$$

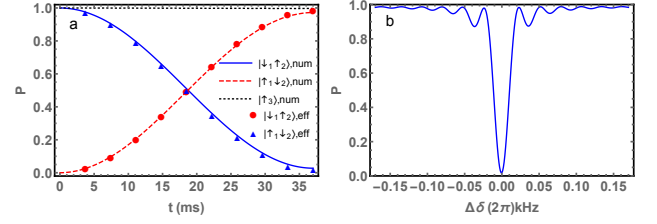


FIG. 2. (a) Comparison of the effective (eff) dynamics under master equation (3) and the exact numerical simulation (num) by using full Hamiltonian equation (2) and NV resets applied every  $T_{1\rho} = t_{re} = 1$  ms. The solid blue (dashed red) curve denotes the probability of measuring  $|\downarrow, \uparrow\rangle$  ( $|\uparrow, \downarrow\rangle$ ) as a function of time  $t$ . Choosing  $\Omega = (2\pi)300$  kHz,  $\gamma_{ni}B_0 = (2\pi)200$  kHz for the NV center, we achieve a near perfect coherent flip-flop between nuclear spins 1 and 2 with  $(a_{\parallel 1}, a_{\perp 1}) = (2\pi)(1.99, 2.01)$  kHz,  $(a_{\parallel 2}, a_{\perp 2}) = (2\pi)(2.00, 5.01)$  kHz that are coupled via the NV spin, while the nuclear spin 3 with  $(a_{\parallel 3}, a_{\perp 3}) = (2\pi)(2.30, 2.01)$  kHz is not affected. (b) The parameters are the same as in (a), with the blue line denoting the occupation probability of the state  $|\downarrow, \uparrow\rangle$  for the evolution time  $T = 37$  ms. The high selectivity is demonstrated by assuming a shift of the detuning of the second spin from the resonance condition, with  $\Delta\delta = \delta_i - \delta_2$ .

and

$$A_{wo} \approx \sum_{i=1,2} \frac{a_{\perp i} a_{\perp j}}{32} \left( \frac{\Delta_{-i}}{\Delta_{-i}^2 + (\frac{\Gamma_N}{2})^2} + \frac{\Delta_{+i}}{\Delta_{+i}^2 + (\frac{\Gamma_N}{2})^2} \right) \quad (6)$$

with  $\Delta_{\pm i} = \Omega \pm (\gamma_{ni}B_0 + \frac{a_{\parallel i}}{2})$ . The virtual NV spin excitation results in an indirect dissipation contribution to Eq. (3),

$$\mathcal{D}_{eff}[\rho_n] \approx \sum_{i,j=1,2} \Gamma_{ij}^{eff} \left( I_i^- \rho_n I_j^+ - \frac{1}{2} \{ I_i^+ I_j^-, \rho_n \}_+ \right),$$

with  $\Gamma_{ij}^{eff} = \sum_{j=1,2} \frac{a_{\perp i} a_{\perp j}}{32} \left( \frac{\Gamma_N}{\Delta_{+j}^2 + (\frac{\Gamma_N}{2})^2} + \frac{\Gamma_N}{\Delta_{-i}^2 + (\frac{\Gamma_N}{2})^2} \right)$ . Notice that the periodic reset of the NV maintains a net NV polarization ( $p > 0$ ), which is critical to our scheme. The NV center provides two channels for virtual electron spin flips, via  $|-_x\rangle$  and  $|+_x\rangle$  [31], that mediate interaction between the nuclei. As the two channels produce effective nuclear couplings with opposing sign, in the absence of periodic reinitialization, the mixing of the two channels would induce no net coherent evolution ( $p = 0$ ) for an evolution time that is longer than the NV lifetime  $T_{1\rho}$  while a net interaction is achieved in the presence of periodic reinitialization ( $p > 0$ ).

*Quantum gate implementation* — The effective coupling term in Eq. (4) gives rise to coherent flip-flop processes between the two nuclear spins, which achieves very high fidelity under the condition  $p A_{wo} \gg \Gamma^{eff}$ . As the effective relaxation rate  $\Gamma^{eff}$  is inversely proportional to the square of the detuning  $\Delta_{\pm i}$ , we can adjust  $\Delta_{\pm i}$  and the NV reset time, i.e., a large detuning  $\Delta_{\pm i} \gg \Gamma_N$  and  $t_{re} \sim T_{1\rho}$  to minimize this induced dissipation. Thus, it is possible to have coherent internuclear evolution well

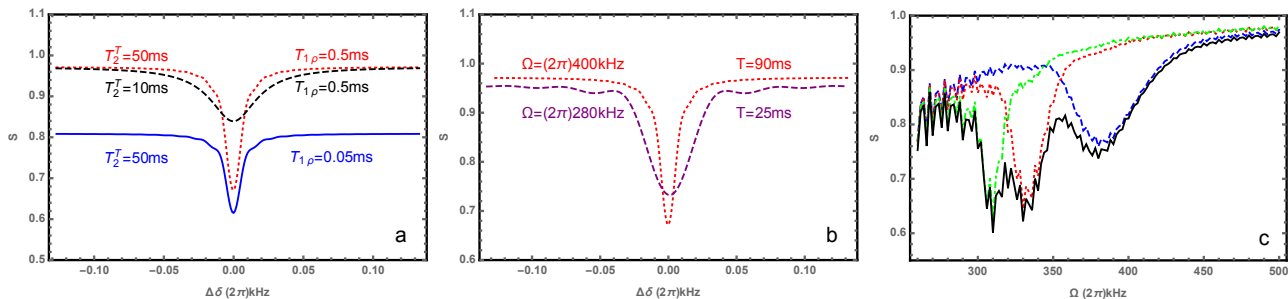


FIG. 3. (a), The effect of the NV  $T_{1\rho}$  and the target spin decoherence time  $T_2^T$  on the detection bandwidth. The sensor signal  $S$  (probability that the sensor spin is found in its initial state) is calculated by exact simulation for a total run time of  $T = 90$  ms and three combinations of  $T_{1\rho}$ ,  $T_2^T$ . The NV spin is reinitialized every  $t_{re} = T_{1\rho}$  and we chose  $\omega_{L1} = (2\pi)200$  kHz,  $\Omega = (2\pi)400$  kHz and couplings  $a_{\perp 1} = (2\pi)10$  kHz for the sensor nucleus and  $a_{\perp 2} = (2\pi)1$  kHz for the target nucleus. It can be seen that only the sensor  $T_2^T$  has an effect on the linewidth, while the NV  $T_{1\rho}$  only affects the signal strength. (b), The tunable NV detuning  $\Delta_{\pm i}$  as a frequency filter - the red dotted line has identical parameters to that in (a), the purple dashed line with different MW Rabi frequency results in smaller detuning which leads to increased linewidth due to increased  $A_{wo}$  and  $\Gamma_{ij}^{eff}$ . (c), Assuming three  $^{13}\text{C}$  nuclear spins in a Valine molecule. The NV spin is at the origin, the sensor at  $[-0.601, 0.676, -0.692]\text{nm}$ , and targets at  $[-1.260, -1.451, 2.904]\text{nm}$ ,  $[-1.260, -1.317, 3.135]\text{nm}$  and  $[-1.260, -1.317, 2.673]\text{nm}$ , with the magnetic field direction  $[44.7^\circ, 52.0^\circ]$  and  $T = 60$  ms. The dashed lines show individual contribution to the NV spin, while the black solid line represents the total signal of the three  $^{13}\text{C}$  spins with different coupling components to the NV spin, while the black solid line represents the total signal of the three  $^{13}\text{C}$  spins with different coupling components to the NV spin, while the black solid line represents the total signal of the three  $^{13}\text{C}$  spins with different coupling components to the NV spin, while the black solid line represents the total signal of the three  $^{13}\text{C}$  spins with different coupling components to the NV spin. The internuclear coupling has been suppressed by means of dynamical decoupling. The small amplitude oscillations on the observed signal are due to off-resonant contributions, which can be suppressed by choosing larger detunings  $\Delta_{\pm i}$ , i.e. larger Rabi frequency  $\Omega$ .

beyond the life time of NV spin. In Fig. 2a, we initialize two nuclear spins in state  $|\downarrow_1\uparrow_2\rangle$  and a third one in state  $|\uparrow_3\rangle$ . The coherent flip-flop interaction between  $|\downarrow_1\uparrow_2\rangle \leftrightarrow |\uparrow_1\downarrow_2\rangle$  induces an nuclear XX gate between the nuclear spins weakly coupled to NV spin with  $T_{1\rho} = 1$  ms. We compute the average fidelity to find 0.994 [34], significantly higher than the fidelity ( $< 0.66$ ) of nuclear-nuclear gates achieved so far with NV centers by using 4 electron-nuclear spin quantum gates (if each fidelity  $< 0.90$  [1]). For the  $^{13}\text{C}$  nuclear spin bath surrounding an NV spin, in principle, one could select two weakly nuclear spins to implement a near perfect quantum gate at room temperature. For quantum registers that are composed of several nuclei, it is important that quantum gates between two spins do not affect the other qubits in the register. As shown in Fig. 2a, our scheme can achieve very high selectivity. Even a 0.3 kHz deviation of the parallel component coupling from the resonance leaves a third nuclear spin unaffected by the quantum gate, see Fig. 2b for the high specificity of the interaction. The resulting spatial resolution will be further discussed later.

*Detection of a single nucleus* — The coupling between the nuclear spins mediated by a dissipative NV can also be used for sensing an isolated single nucleus outside of the diamond. Our scheme includes three steps: (1), Polarize the  $^{13}\text{C}$  nuclear sensor spin by using the NV center electron spin. (2), Achieve polarisation transfer via a frequency selective flip-flop process between the two nuclear spins that is mediated by a dissipative NV center. (3), Use NV center to read out the polarization leakage of the nuclear  $^{13}\text{C}$  spin sensor, which indicates the existence of a distant nuclear spin at the selected frequency.

The electron spin of the NV center can be optically initialized and read out by using laser illumination. The nearby nuclear  $^{13}\text{C}$  sensor spin can also be well-controlled by a SWAP gate between NV and nuclear spin, i.e., it can be polarized and its position can be detected. A high-fidelity SWAP operation can be constructed by using radio-frequency (rf) and MW pulses [22, 35] or via the use of decoherence protected gates [36].

Therefore if the sensor  $^{13}\text{C}$  spin is polarized to the ground state  $|\downarrow_1\rangle$ , we can detect the target  $^{13}\text{C}$  nuclear spin by sensing the polarization leakage of the sensor. After time  $t$ , we measure the probability that the sensor  $^{13}\text{C}$  spin remains in the state  $|\downarrow_1\rangle$  which depends on the effective internuclear coupling strength  $A_{wo}$  as follows

$$S = 1 - \frac{(pA_{wo})^2 \sin^2(\frac{t}{2} \sqrt{(pA_{wo})^2 + (\delta_1 - \delta_2)^2})}{2[(pA_{wo})^2 + (\delta_1 - \delta_2)^2]}. \quad (7)$$

It is easy to find the resonance condition  $\delta_1 = \delta_2$ . In our setup, the coupling of the nuclear sensor (which is labeled spin 1 and whose position can be determined precisely) to the NV is far larger than that of the nuclear target to the NV. In order to match the resonance condition to the target nuclear spin, two main degrees of freedom are available- we can adjust the direction of the magnetic field which gives a coarse tuning, and the Rabi frequency of the microwave drive on the NV spin, which allows a fine-tuning to match the resonance condition [31]. Note that the Rabi frequency has only second order contributions to the resonance condition, i.e.,  $\frac{a_{\perp i}^2}{16\Delta_{\pm i}}$ , thus our scheme is not sensitive to small deviations or fluctuations of the Rabi frequency. Once the resonance condition is achieved, the signal dips around the time  $t = \pi/4pA_{wo}$

marking the presence of nuclear spin.

*Enhanced spatial resolution* — When using the NV as a sensor by observing the polarization leakage from the NV center to the nuclear spins [37], there exist two major limitations for the frequency resolution: that the NV  $T_1^\rho$  relaxation has to be longer than the NV-nuclear flip-flop time and the requirement that the hyperfine transverse component is small ( $|a_{\parallel i} - a_{\parallel j}|/2 > a_{\perp i/j}$ ). Our scheme solves both of these limitations. First, in our scheme the influence of NV decoherence ( $T_2$ ) and relaxation ( $T_1$ ) on the dynamics can be reduced at will below any desired level by increasing detuning  $\delta_{\pm i}$  and NV reset rate. Therefore the resolution is limited only by the target spin decoherence  $T_2^T$  (see Fig. 3a). Second, the broadening due to  $a_{\perp i}$  now depends quadratically on  $a_{\perp i}$  (see Eq. (5)) and is essentially proportional to the effective coupling  $pA_{wo}$  (see Eq. (6)), which is at least one order of magnitude smaller than  $a_{\perp i/j}$ . Thus the frequency resolution is improved accordingly as we now need to require  $|\delta_i^w - \delta_j^w| \simeq |a_{\parallel i} - a_{\parallel j}|/2 > pA_{wo}$ . Moreover, increasing the detuning  $\Delta_{\pm i}$  of the NV induces a smaller effective coupling  $pA_{wo}$  enhancing the frequency resolution (see Fig. 3b), which also gives a tunable frequency filter. For optimal resolution, one would fix the NV detuning  $\Delta_{\pm i}$  to balance the two limitations, i.e.  $\frac{1}{pA_{wo}} \lesssim T_2^T$ . For example, for  $T_{1\rho} = 0.05$  ms and  $T_2^T = 50$  ms, the resolution could be improved a thousand-fold compared to direct sensing via the NV center spin.

Recently the use of a nuclear spin as ancillary memory to enhance the resolution of NV detection has been proposed for correlation spectroscopy [19, 23, 24]. However, the enhanced spectral resolution is offset by other disadvantages, not present in our proposed scheme, which are especially limiting for the regime of interest in NV sensing, i.e. an NV  $\sim 3 - 5$  nm from the surface, attempting to sense single nuclear spins ( $a_{\perp} \approx 1$  kHz). In correlation spectroscopy the interaction time with the target nuclei is limited by the  $T_2^{NV}$  of the NV, while the longest time interval between interrogations, and hence the spectral resolution, is limited by the  $T_2^{ancilla}$  time of the nuclear ancilla. Therefore, the SNR for a given unit time is reduced by a factor of  $T_2^{NV}/T_2^{ancilla} < 0.01$  due to the relatively long "dead-time" in between measurements. Ramsey spectroscopy [5] by using an NV-center is limited due to the required initialization and the read-out of the nuclear spin. The efficient initialization of the nuclear spin requires  $a_{\perp}T_2^{NV} \ll 1$  and spectrally selective addressing is limited by  $T_2^{NV}$ . In correlation spectroscopy the SNR is reduced due to long time interval between measurements. In contrast, in our set-up it is the nuclear spin which serves directly as a sensor which is not limited by the decoherence and relaxation of the NV spin. One can estimate the sensitivity of our scheme as follows: suppose  $t_{re} = T_{1\rho}$ , as both  $\sqrt{1/\Gamma_{eff}}$  and  $pA_{wo}$  are linearly dependent on the detunings  $\Delta_{\pm i}$ , the sensitivity per unit time of our scheme is proportional to  $\frac{pA_{wo}}{\sqrt{1/\Gamma_{eff}}} \sim \frac{a_{\perp 2}^4}{\sqrt{T_{1\rho}}}$ , which is independent of  $\Delta_{\pm i}$ . This is

of the same order as the sensitivity achieved by direct detection of a nucleus by polarisation leakage of the NV [37] while obtaining enhanced spectral resolution. Therefore, our scheme achieves the enhanced resolution without a penalty to the sensitivity, and the scheme validity does not suffer from nearby nuclear spins or relatively low coupling to the nuclear spins.

*Sensing application* — To evaluate the effectiveness of our scheme, we use it to determine the molecular structure of a simple target molecule. To sense and address individual nuclear spins in a crowded cluster in the molecule, the internuclear dipolar coupling needs to be suppressed which we achieve by application of the WAHUA [38] decoupling sequences during the evolution. This sequence averages the internuclear dipolar coupling to zero over the cycle time, at the cost of a reduction factor in the dipolar coupling strength  $1/\sqrt{3}$ . Consider as an example the molecule malic acid (Valine), which plays an important role in biochemistry and is not too large to prevent exact numerical simulations. In Fig. 3c, we simulate the case of three  $^{13}\text{C}$  spins in this molecule, attached to the diamond about 3.9 nm from the NV spin. The 1D NMR spectra show the information on the dipolar coupling to the nuclear spins. The dip height depends on the transverse coupling, as we have  $S^d = 1 - \frac{1}{2}\sin^2(pA_{wo}T/2)$  with  $T$  the evolution time, and the longitudinal dipolar coupling can be derived from the energy matching condition, which gives a pair of parameters  $a_{\parallel 2}$  and  $a_{\perp 2}$ . Although 1D NMR spectra is not sufficient for determination of the position of the target without extra chemical information, one can adjust the magnetic field orientation to determine precisely the 3D position of nuclear spins in the molecule. Due to continuous collection of the signal, only a small number of measurements repetitions are required to reach the SNR threshold. Assuming  $C \approx 0.2$  is the combined contrast and photon collection efficiency, and we ignore the time for initialization of our setup and the SWAP gates are ignored here because of small values then, with  $pA_{wo} \sim (2\pi)16$  Hz and  $T = 60$  ms, we estimate that the experimental time for registering one dip in Fig. (3c) is about 1.8 s, assuming that we take measurements for 15 frequency steps.

*Conclusion* — We have designed a method that achieves the coupling between distant nuclear spins mediated by a dissipatively decoupled electron spin of an NV center which suppresses the impact of NV decoherence and relaxation processes on these nuclei. This enables high fidelity selective quantum gates between two weakly coupled nuclear spins in a quantum register at ambient condition. Importantly for sensing applications, our method enables the direct use of a nuclear spin as a quantum sensor rather than merely as a memory. The controllable second-order coupling provides a tunable and sharp frequency filter for collecting the signal continuously, hence increasing the SNR, while remaining insensitive to decoherence and relaxation of the mediating NV. Therefore, making use of dissipation as a tool, the pro-

posed NV-mediated scheme increases the ability of detection and coherence control of nuclear spins as well as analysis of complex spin structures.

*Acknowledgements* — The authors thank L. McGuinness and Zhenyu Wang for helpful discussions and ad-

vice. This work was supported by the ERC Synergy grant BioQ, the EU projects DIADEMS, HYPERDIAMOND and EQUAM, the DFG CRC/TRR 21 and an Alexander von Humboldt Professorship.

- 
- [1] T. H. Taminiau, J. Cramer, T. van der Sar, V. V. Dobrovitski, and R. Hanson, “Universal control and error correction in multi-qubit spin registers in diamond,” *Nature nanotechnology*, vol. 9, no. 3, pp. 171–176, 2014.
- [2] G. Waldherr, Y. Wang, S. Zaiser, M. Jamali, T. Schulte-Herbrüggen, H. Abe, T. Ohshima, J. Isoya, J. Du, P. Neumann *et al.*, “Quantum error correction in a solid-state hybrid spin register,” *Nature*, vol. 506, no. 7487, pp. 204–207, 2014.
- [3] J. Casanova, Z.-Y. Wang, and M. B. Plenio, “Noise-resilient quantum computing with a nitrogen-vacancy center and nuclear spins,” *Phys. Rev. Lett.*, vol. 117, p. 130502, Sep 2016.
- [4] A. Bermudez, F. Jelezko, M. B. Plenio, and A. Retzker, “Electron-mediated nuclear-spin interactions between distant nitrogen-vacancy centers,” *Physical review letters*, vol. 107, no. 15, p. 150503, 2011.
- [5] G. Waldherr, J. Beck, P. Neumann, R. Said, M. Nitsche, M. Markham, D. Twitchen, J. Twamley, F. Jelezko, and J. Wrachtrup, “High-dynamic-range magnetometry with a single nuclear spin in diamond,” *Nature nanotechnology*, vol. 7, no. 2, pp. 105–108, 2012.
- [6] T. H. Taminiau, J. J. T. Wagenaar, T. Van der Sar, F. Jelezko, V. V. Dobrovitski, and R. Hanson, “Detection and control of individual nuclear spins using a weakly coupled electron spin,” *Physical review letters*, vol. 109, no. 13, p. 137602, 2012.
- [7] S. Kolkowitz, Q. P. Unterreithmeier, S. D. Bennett, and M. D. Lukin, “Sensing distant nuclear spins with a single electron spin,” *Physical review letters*, vol. 109, no. 13, p. 137601, 2012.
- [8] N. Zhao, J. Honert, B. Schmid, M. Klas, J. Isoya, M. Markham, D. Twitchen, F. Jelezko, R.-B. Liu, H. Fedder *et al.*, “Sensing single remote nuclear spins,” *Nature nanotechnology*, vol. 7, no. 10, pp. 657–662, 2012.
- [9] S. Kaufmann, D. A. Simpson, L. T. Hall, V. Perunicic, P. Senn, S. Steinert, L. P. McGuinness, B. C. Johnson, T. Ohshima, F. Caruso *et al.*, “Detection of atomic spin labels in a lipid bilayer using a single-spin nanodiamond probe,” *Proceedings of the National Academy of Sciences*, vol. 110, no. 27, pp. 10894–10898, 2013.
- [10] A. Ermakova, G. Pramanik, J.-M. Cai, G. Algara-Siller, U. Kaiser, T. Weil, Y.-K. Tzeng, H. C. Chang, L. P. McGuinness, M. B. Plenio *et al.*, “Detection of a few metallo-protein molecules using color centers in nanodiamonds,” *Nano letters*, vol. 13, no. 7, pp. 3305–3309, 2013.
- [11] H. J. Mamin, M. Kim, M. H. Sherwood, C. T. Rettner, K. Ohno, D. D. Awschalom, and D. Rugar, “Nanoscale nuclear magnetic resonance with a nitrogen-vacancy spin sensor,” *Science*, vol. 339, no. 6119, pp. 557–560, 2013.
- [12] T. Staudacher, F. Shi, S. Pezzagna, J. Meijer, J. Du, C. A. Meriles, F. Reinhard, and J. Wrachtrup, “Nuclear magnetic resonance spectroscopy on a (5-nanometer) 3 sample volume,” *Science*, vol. 339, no. 6119, pp. 561–563, 2013.
- [13] M. Grinolds, M. Warner, K. De Greve, Y. Dovzhenko, L. Thiel, R. L. Walsworth, S. Hong, P. Maletinsky, and A. Yacoby, “Subnanometre resolution in three-dimensional magnetic resonance imaging of individual dark spins,” *Nature nanotechnology*, vol. 9, no. 4, pp. 279–284, 2014.
- [14] C. Müller, X. Kong, J.-M. Cai, K. Melentijević, A. Stacey, M. Markham, D. Twitchen, J. Isoya, S. Pezzagna, J. Meijer *et al.*, “Nuclear magnetic resonance spectroscopy with single spin sensitivity,” *Nature communications*, vol. 5, no. 4703, 2014.
- [15] A. Sushkov, I. Lovchinsky, N. Chisholm, R. L. Walsworth, H. Park, and M. D. Lukin, “Magnetic resonance detection of individual proton spins using quantum reporters,” *Physical review letters*, vol. 113, no. 19, p. 197601, 2014.
- [16] F. Shi, Q. Zhang, P. Wang, H. Sun, J. Wang, X. Rong, M. Chen, C. Ju, F. Reinhard, H. Chen *et al.*, “Single-protein spin resonance spectroscopy under ambient conditions,” *Science*, vol. 347, no. 6226, pp. 1135–1138, 2015.
- [17] L. Trifunovic, F. L. Pedrocchi, S. Hoffman, P. Maletinsky, A. Yacoby, and D. Loss, “High-efficiency resonant amplification of weak magnetic fields for single spin magnetometry at room temperature,” *Nature nanotechnology*, vol. 10, no. 6, pp. 541–546, 2015.
- [18] I. Lovchinsky, A. O. Sushkov, E. Urbach, N. de Leon, S. Choi, K. De Greve, R. Evans, R. Gertner, E. Bersin, C. Müller *et al.*, “Nuclear magnetic resonance detection and spectroscopy of single proteins using quantum logic,” *Science*, vol. 351, no. 6275, pp. 836–841, 2016.
- [19] A. Laraoui, F. Dolde, C. Burk, F. Reinhard, J. Wrachtrup, and C. A. Meriles, “High-resolution correlation spectroscopy of  $^{13}\text{C}$  spins near a nitrogen-vacancy centre in diamond,” *Nature communications*, vol. 4, p. 1651, 2013.
- [20] A. Ajoy, U. Bissbort, M. D. Lukin, R. L. Walsworth, and P. Cappellaro, “Atomic-scale nuclear spin imaging using quantum-assisted sensors in diamond,” *Physical Review X*, vol. 5, no. 1, p. 011001, 2015.
- [21] J. N. Greiner, D. D. B. Rao, P. Neumann, and J. Wrachtrup, “Indirect quantum sensors: improving the sensitivity in characterizing very weakly coupled spins,” *Faraday discussions*, vol. 184, pp. 163–171, 2015.
- [22] Z.-Y. Wang, J. Casanova, and M. B. Plenio, “Delayed entanglement echo for individual control of a large number of nuclear spins,” *arXiv preprint arXiv:1604.05731*, 2016.
- [23] S. Zaiser, T. Rendler, I. Jakobi, T. Wolf, S.-Y. Lee, S. Wagner, V. Bergholm, T. Schulte-Herbrüggen, P. Neumann, and J. Wrachtrup, “Enhancing quantum sensing sensitivity by a quantum memory,” *Nature Communications*, vol. 7, 2016.
- [24] M. Pfender, N. Aslam, H. Sumiya, S. Onoda, P. Neu-

- mann, J. Isoya, C. Meriles, and J. Wrachtrup, “Non-volatile quantum memory enables sensor unlimited nanoscale spectroscopy of finite quantum systems,” *arXiv preprint arXiv:1610.05675*, 2016.
- [25] T. Rosskopf, J. Zopes, J. Boss, and C. Degen, “A quantum spectrum analyzer enhanced by a nuclear spin memory,” *arXiv preprint arXiv:1610.03253*, 2016.
- [26] S. Schmitt, T. Gefen, F. M. Stürmer, T. Unden, G. Wolff, C. Müller, J. Scheuer, B. Naydenov, M. Markham, S. Pezzagna, J. Meijer, I. Schwarz, M. B. Plenio, A. Retzker, L. P. Mc Guinness, and F. Jelezko, “Sub-millihertz magnetic spectroscopy with a nanoscale quantum sensor,” *Submitted*, 2016.
- [27] A. Ajoy, Y. Liu, and P. Cappellaro, “Dc magnetometry at the  $t_2$  limit,” *arXiv preprint arXiv:1611.04691*, 2016.
- [28] A. Bermudez, T. Schätz, and M. B. Plenio, “Dissipation-assisted quantum information processing with trapped ions,” *Physical review letters*, vol. 110, p. 110502, 2013.
- [29] M. Kost, J. M. Cai, and M. B. Plenio, “Resolving single molecule structures with nitrogen-vacancy centers in diamond,” *Scientific Reports*, vol. 5, p. 11007, 2015.
- [30] J. Scheuer, A. Stark, M. Kost, M. B. Plenio, B. Naydenov, and F. Jelezko, “Accelerated 2d spectroscopy of single spins using matrix completion,” *Scientific Reports*, vol. 5, p. 17728, 2015.
- [31] See supplemental material.
- [32] C. Cohen-Tannoudji, J. Dupont-Roc, G. Grynberg, and P. Thickstun, *Atom-photon interactions: basic processes and applications*. Wiley Online Library, 1992.
- [33] J. R. Schrieffer and P. A. Wolff, “Relation between the anderson and kondo hamiltonians,” *Physical Review*, vol. 149, no. 2, p. 491, 1966.
- [34] M. A. Nielsen, “A simple formula for the average gate fidelity of a quantum dynamical operation,” *Physics Letters A*, vol. 303, no. 4, pp. 249–252, 2002.
- [35] L. Jiang, J. S. Hodges, J. R. Maze, P. Maurer, J. M. Taylor, D. G. Cory, P. R. Hemmer, R. L. Walsworth, A. Yacoby, A. S. Zibrov *et al.*, “Repetitive readout of a single electronic spin via quantum logic with nuclear spin ancillae,” *Science*, vol. 326, no. 5950, pp. 267–272, 2009.
- [36] P. Cappellaro, L. Jiang, J. S. Hodges, and M. D. Lukin, “Coherence and control of quantum registers based on electronic spin in a nuclear spin bath,” *Physical review letters*, vol. 102, no. 21, p. 210502, 2009.
- [37] J. Cai, F. Jelezko, M. B. Plenio, and A. Retzker, “Diamond-based single-molecule magnetic resonance spectroscopy,” *New Journal of Physics*, vol. 15, no. 1, p. 013020, 2013.
- [38] J. S. Waugh, L. M. Huber, and U. Haeberlen, “Approach to high-resolution nmr in solids,” *Physical Review Letters*, vol. 20, no. 5, p. 180, 1968.